HHS Public Access

Author manuscript

Mol Pharm. Author manuscript; available in PMC 2020 January 01.

Published in final edited form as:

Mol Pharm. 2019 July 01; 16(7): 2858–2871. doi:10.1021/acs.molpharmaceut.8b01284.

Development of liposomal gemcitabine with high drug loading capacity

Tamam Hassan[1,2], **Park Jinho**[2], **Gadalla Hytham H.**[2,3], **Andrea R. Masters**[4], **Jelan A. Abdel-Aleem**[1], **Sayed I. Abdelrahman**[1], **Aly A. Abdelrahman**[1], **L. Tiffany Lyle**[5], **Yoon Yeo**[2,6,*]

[1]Department of Industrial Pharmacy, Faculty of Pharmacy, Assiut University, Assiut 71526, Egypt

[2]Department of Industrial and Physical Pharmacy, Purdue University, 575 Stadium Mall Drive, West Lafayette, IN 47907, USA

[3]Department of Pharmaceutics, Faculty of Pharmacy, Assiut University, Assiut 71526, Egypt

[4]Clinical Pharmacology Analytical Core, Indiana University Melvin and Bren Simon Cancer Center, Indiana University School of Medicine, Indianapolis, IN 46202, USA

[5]Department of Comparative Pathobiology, Purdue University, West Lafayette, IN 47907, USA

[6]Weldon School of Biomedical Engineering, Purdue University, West Lafayette, IN 47907, USA

Abstract

Liposomes are widely used for systemic delivery of chemotherapeutic agents to reduce their nonspecific side effects. Gemcitabine (Gem) makes a great candidate for liposomal encapsulation due to the short half-life and non-specific side effects; however, it has been difficult to achieve liposomal Gem with high drug loading capacity. Remote loading, which uses a transmembrane pH gradient to induce influx of drug and locks the drug in the core as a sulfate complex, does not serve Gem as efficiently as doxorubicin (Dox) due to the low pKa value of Gem. Existing studies have attempted to improve Gem loading capacity in liposomes by employing lipophilic Gem derivatives or creating a high concentration gradient for active loading into the hydrophilic cores (small volume loading). In this study we combine remote loading approach and small volume loading or hypertonic loading, a new approach to induce the influx of Gem into the preformed liposomes by high osmotic pressure, to achieve a Gem loading capacity of 9.4 – 10.3 wt% in contrast to 0.14 – 3.8 wt% of the conventional methods. Liposomal Gem showed a good stability during storage, sustained-release over 120 h in vitro, enhanced cellular uptake and improved cytotoxicity as compared to free Gem. Liposomal Gem showed a synergistic effect with liposomal Dox on Huh7 hepatocellular carcinoma cells. A mixture of liposomal Gem and liposomal Dox delivered both drugs to the tumor more efficiently than a free drug mixture and showed a relatively good anti-tumor effect in a xenograft model of hepatocellular carcinoma. This study shows that

*Corresponding author: Yoon Yeo, Ph.D., Phone: 1.765.496.9608, Fax: 1.765.494.6545, yyeo@purdue.edu.

Supporting Information

Comparison of Gem-loaded liposomes (Supporting table); schematic of remote loading and pH-dependent drug release of liposomal Dox; drug release kinetics of drug-coloaded liposomes; cytotoxicity of blank liposomes; flow cytometry analysis of Huh 7 cells incubated with Dox and L_RD; HPLC chromatographs of representative in vivo analytes; weight change of animals receiving PBS, free drug mixture, or liposomal mixture; TUNEL assay of tumor sections; and histological evaluation of major organs (Supporting figures)

bioactive liposomal Gem with high drug loading capacity can be produced by remote loading combined with additional approaches to increase drug influx into the liposomes.

Keywords

Liposomes; drug loading capacity; gemcitabine; small volume loading; hypertonic loading; remote loading

1. Introduction

Liposomal drug carriers are used to reduce non-specific side effects of systemic chemotherapy. An important feature of liposomes is the versatility: liposomes can carry both hydrophilic and lipophilic drugs, with the former in the aqueous core compartment and the latter in the lipid bilayer membrane, respectively. Hydrophilic drugs can be passively loaded in the aqueous core during the hydration of the lipid film as part of the hydrating medium. Alternatively, weak acid or base drugs can be brought into the core compartment of preformed liposomes via chemical gradients across the lipid bilayer.[1, 2] In case of base drugs, liposomes are filled with ammonium salts of sulfate, citrate, phosphate, or acetate, which ionize to ammonium and the counterions.[3] The ammonium further dissociates to ammonia and proton, where the former with relatively high transmembrane diffusivity moves out of the liposomes leaving behind protons with lower diffusivity.[1] The differential transmembrane diffusivity results in the acidification of the liposome interior, inducing ionization of the drug and its complexation with counterions, which forms a membrane-impermeable ionic drug complex. A high concentration gradient of free drug, thereby formed, induces the influx of a drug into the liposomes (Supporting Fig. 1a). This method, called ‘remote loading’, has been employed in liposomal formulations of doxorubicin (Dox),[4] bringing significant improvement in pharmacokinetics and safety profiles of the drug in humans.[4–6]

While the remote loading method can encapsulate drugs with a higher loading capacity (drug to liposome weight ratio) than the passive loading, it does not work for all the weak acid or base drugs. Gemcitabine (Gem), a prodrug of 2’,2’-difluorodeoxycytidine 5’-triphosphate (dFdCTP) serving as a competitive inhibitor of dCTP in DNA polymerization,[7] is an exemplary drug that is difficult to encapsulate in liposomes. As a weak base, Gem can form an ionic complex with sulfate but not encapsulated in liposomes as efficiently as Dox by the remote loading method.[8] Gem with a pKa value of pH 3.6 does not ionize in the acidic aqueous compartment of liposomes as extensively as Dox (pKa: pH 8.68); thus, the pH gradient across the membrane does not translate to a high concentration gradient of unionized Gem.[8] Therefore, the maximum loading capacity of Gem that can be achieved by the remote loading is no higher than 1 wt%.[8, 9] The low drug loading capacity is problematic for several reasons. First of all, a large loss of drug during the preparation is not economical.[4] Secondly, inefficient drug loading necessitates the use of a large amount of polar lipids that may cause unintended biological effects.[10] Moreover, the increased total dose due to the low drug loading increases the injection volume and/or the concentration of liposomes to the extent that they become the dose-limiting factors.[11, 12] A large dose of liposomes has also

met with an increased toxicity in mice, due to the delayed tissue distribution of liposomes accompanied by the extended circulation, which increases the chances of free drug leakage.[13]

Consistent with the difficulty in efficient loading, no viable liposomal Gem product is currently available on the market. Nevertheless, there are several compelling reasons to develop liposomal Gem. Upon systemic administration, Gem undergoes rapid metabolism and renal clearance with a half-life of 8–17 min.[14] Non-specific distribution of Gem induces serious side effects such as myelosuppression, neutropenia, thrombocytopenia, and anemia.[15] Liposomal Gem has the potential to improve the bioavailability and safety of Gem. Moreover, Gem is broadly pursued as a combination therapy with Dox in the treatment of breast cancer[16, 17] and hepatocellular carcinoma[18, 19] for a synergistic effect.[20–25] Liposomal Gem will be a more effective counterpart of liposomal Dox in achieving co-localization of the drug combination. Therefore, there is a strong unmet need for efficient liposomal encapsulation of Gem.

An approach to improve liposomal encapsulation of Gem involves the incubation of preformed liposomes in a small volume of concentrated Gem solution, which keeps the external Gem at the saturation solubility and thus generates the maximum concentration gradient across the liposomal membrane.[8] With the small volume loading method, the loading capacity of Gem in the liposomes increased from 0.2 wt% to 4 wt%.[8] Another approach uses lipophilic Gem prodrugs, such as valeroyl, heptanoyl, lauroyl and stearoyl linear acyl derivatives of Gem, for liposomal encapsulation, achieving a loading capacity of up to 24 mol% (8.6 wt% as Gem).[26]

In this study, we explore various strategies to further increase Gem loading in liposomes, including a new method, called *hypertonic loading*. This simple method utilizes high osmotic pressure across the lipid bilayer, which induces the influx of external water phase containing unionized Gem. The hypertonic loading and small volume loading methods are combined with remote loading to reduce the back diffusion of Gem from liposomes. The optimized liposomal Gem is characterized with respect to the physicochemical properties and in vitro activities, as compared with liposomal Dox. The in vivo efficacy of liposomal Gem is tested in the context of combination therapy with liposomal Dox in a xenograft model of Huh7 hepatocellular carcinoma.

2. Materials and Methods

2.1. Materials

Dipalmitoyl-sn-glycero-3-phosphocholine (DPPC), cholesterol and N-(carbonyl-methoxypolyethylene-glycol-2000)-1, 2-distearoyl-sn-glycero-3-phospho-ethanolamine (DSPE-PEG_{2000}) were purchased from Avanti Polar Lipids (Alabaster, AL). Gemcitabine (Gem) and Doxorubicin HCl (Dox) were purchased from LC laboratories (Woburn, MA). Gemcitabine-5’-triphosphate (2’,2’-difluorodeoxycytidine 5’-triphosphate, dFdCTP) was purchased from Sierra Bioresearch (Tucson, AZ). 3-(4,5-dimethylthiazol-2-yl)-2,5-diphenyltetrazolium bromide (MTT) was purchased from Invitrogen (Carlsbad, CA). Terminal deoxynucleotidyl transferase dUTP nick end labeling kit (DeadEnd Fluorometric

TUNEL System) was purchased from Promega (Madison, WI). All other materials, including solvents, were purchased from Sigma Aldrich (St. Louis, MO).

2.2. Liposome preparation

Liposomes were prepared in the following procedure with variations in hydration and drug loading methods (Fig. 1). A mixture of DPPC, cholesterol, DSPE-PEG_{2000} at a weight ratio of 6:3:1 (20 mg in total) was dissolved in 3 mL of a 3:1 mixture of chloroform and methanol. For the preparation of fluorescently-labeled liposomes, 1 mg of cholesterol was replaced with 25-NBD cholesterol. A thin lipid film was obtained by removing the solvents with a rotary evaporator at 45 °C and hydrated according to the procedures detailed below. The hydrated lipid film was sonicated in a sonic water bath (Bransonic ultrasonic Co, Danbury, CT) for 15 min and extruded through polycarbonate membranes with a pore size of 400 nm and 200 nm, sequentially, using a Mini-extruder (Avanti polar lipid, Inc., AL). The drug-loaded liposomes were washed with deionized (DI) water 3 times by ultracentrifugation at 135,700 rcf at 4 °C and used as is unless specified otherwise. No drug was detectable in the supernatant collected after the 3rd centrifugation, which confirmed the complete removal of unencapsulated drug. In all methods, each batch used 20 mg of lipid components and 5 mg of Gem and/or 5 mg of Dox (theoretical loading capacity of 20 wt%).

Passive loading: The lipid film was hydrated with 1 mL of 5 mg/mL Gem solution and stirred in a rotary evaporator for 45 min at 45 °C, extruded and washed as described above. The Gem-loaded liposomes prepared by this method are called L_PG.

Remote loading: The lipid film was hydrated 1.2 mL of 250 mM ammonium sulfate solution and stirred in a rotary evaporator for 60 min at 45°C. The hydrated film was bath sonicated, extruded and collected by centrifugation at 305,400 rcf. The liposomal pellet was dispersed in 0.5 mL of 10 mg/mL Gem or Dox solution by bath sonication and incubated at 60 °C overnight. The liposomes were then washed as described above. The Gem- or Dox-loaded liposomes prepared by remote loading are called L_RG and L_RD.

Small volume loading[27]: The lipid film was hydrated in 1.2 mL of phosphate-buffered saline (PBS, pH 7.4). The hydrated film was bath sonicated for 10 min, extruded and collected by centrifugation at 305,400 rcf. The liposomal pellet was mixed with 0.1 mL of DI water containing 5 mg of Gem by 15 min bath sonication, followed by overnight incubation at 60 °C. The liposomes were then washed as described above. The Gem-loaded liposomes prepared by small volume loading are called L_SG.

Hypertonic loading: The lipid film was hydrated in 1.2 mL of 462 mM sodium chloride solution. The hydrated film was bath sonicated, extruded and collected by centrifugation at 305,400 rcf. The liposomal pellet was incubated in 0.5 mL of DI water containing 5 mg of Gem at 60 °C overnight. The liposomes were then washed as described above. The Gem-loaded liposomes prepared by hypertonic loading are called L_HG.

Combination of Remote loading and Small volume loading: The liposomal pellet prepared by the remote loading method was mixed with 0.1 mL of DI water containing 5 mg

of Gem by 15 min bath sonication, followed by overnight incubation at 60 °C. The liposomes were then washed as described above. The Gem-loaded liposomes prepared by the combination of remote loading and small volume loading are called $L_{RS}G$. Gem/Dox-coloaded liposomes ($L_{RS}GD$) were prepared by incubating the pellet in 0.1 mL of DI water containing 5 mg Gem and 5 mg Dox at 60 °C overnight.

Combination of Remote loading and Hypertonic loading: The lipid film was hydrated in 1.2 mL of DI water containing 250 mM Ammonium sulfate and 462 mM of sodium chloride. The liposomal pellet was incubated in 0.5 mL DI water containing 5 mg of Gem at 60 °C overnight. The liposomes were then washed as described above. The Gem-loaded liposomes prepared by the combination of remote loading and hypertonic loading are called $L_{RH}G$.

2.3. Liposome characterization

The z-average and zeta potential of each liposomal formulation were measured by a Malvern Zetasizer Nano ZS90 (Worcestershire, UK), as dispersed in DI water (z-average) or in 1 mM phosphate buffer (pH 7.4) (zeta potential). The liposomes were observed by the Tecnai F20 transmission electron microscope (FEI, Hillsboro, OR) after negative staining with 1% uranyl acetate (Gem-loaded liposomes) or 1% phosphotungstic acid (Dox- or co-loaded liposomes). The size of particles in each micrograph was estimated by NIH ImageJ software (Bethesda, MD).

2.4. Drug loading capacity

The purified liposomes were lyophilized, accurately weighed, dispersed in 1 mL of acetonitrile and bath-sonicated in cold water for 2 h. The suspension was diluted with an equal volume of DI water and centrifuged at 16100 rcf for 20 min to obtain a clear supernatant. The supernatant was filtered through a 0.45 μm syringe filter and analyzed by high-pressure liquid chromatography (HPLC). HPLC analysis was performed by the Agilent 1100 system (Agilent Technologies, Palo Alto, CA), equipped with a C18 column (25 cm × 4.6 mm, particle size 5 μm) (Supelco, St. Louis, MO). Dox was eluted with a 70:30 mixture of water and acetonitrile with 0.1% trifluoroacetic acid at a flow rate of 0.8 mL/min and detected at 369 nm.[28] Gem was eluted with a 90:10 mixture of water and acetonitrile at a flow rate of 1 mL/min and detected at 269 nm.[29] The drug loading capacity (%) is defined as $W_D/W_L \times 100$, where W_D is the amount of drug detected and W_L the total amount of drug-loaded liposomes analyzed.

2.5. *In vitro* release kinetics of drug-loaded liposomes

Liposomes equivalent to 115 μg/mL of Gem or 250 μg/mL of Dox were placed in a Float-A-Lyzer G2 dialysis device (Spectrum Laboratories, Inc., Rancho Dominguez, CA) with a molecular weight cut-off of 100 kDa. The device was incubated in 20 mL of PBS (pH 7.4 or pH 5.5) at 37 °C with constant agitation. At predetermined time points, 0.3 mL of the release medium was sampled and replaced with 0.3 mL of fresh buffer. The sampled buffer was filtered with a syringe filter (0.45 μm pore size) and analyzed by HPLC.

2.6. Cytotoxicity of drug-loaded liposomes

Huh7 human hepatocellular carcinoma cells (donation of Prof. Wanqing Liu) were cultured in RPMI-1640 medium complemented with 10% FBS, 100 U/mL penicillin, and 100 μg/mL streptomycin at 37 °C in a humidified 5% CO_2 atmosphere. Huh7 cells were seeded in a 96 well plate at a density of 10,000 cells per well and grown to 70% confluence. Huh7 cells were exposed to free drug or liposomal preparations for 3 or 6 h. The cells were rinsed twice with fresh medium and kept in drug-free medium for 72 h. In another experiment, Huh7 cells were incubated with a free Gem, $L_{RS}G$, $L_{RH}G$, free Dox, L_RD, blank liposomes, free drug mixture, or liposome mixture for 72 h. The medium was then removed, and 15 μL of 5 mg/mL MTT solution and 100 μL media were added to each well and incubated for 4 h at 37 °C. Each well was then treated with 100 μL of stop/solubilization solution and agitated at 37 °C overnight. The absorbance of dissolved formazan was measured at 562 nm by a SpectraMax M3 microplate reader (Molecular Devices, Sunnyvale, CA).

2.7. Determination of optimal sequence of combination treatments

For determination of the optimal sequence of drug treatments, the cells were incubated with free Gem on the first day and free Dox on the second day (or vice versa), with the third day in drug-free medium (*Gem → Dox* or *Dox → Gem*). Alternatively, the cells were incubated with a Gem/Dox on the first day followed by 2 d incubation in drug-free medium (*Gem + Dox*). MTT assay was performed after the three days. The half maximal inhibitory concentration (IC_{50}) of each treatment was determined by GraphPad prism 7 (San Diego, CA). The combination index (CI) of each treatment was determined by Compusyn (Combosyn, Inc., Paramus, NJ). The values of CI < 1, CI = 1, and CI > 1 represent synergy, additivity, and antagonism, respectively.[30]

2.8. Cellular uptake of drug-loaded liposomes

2.8.1. Quantitative analysis—Huh7 Cells were seeded in a 12 well plate at a density of 10^5 cells per well. After overnight incubation, the cells were treated with $L_{RH}G$, $L_{RS}G$, or free Gem at a concentration equivalent to 50 μM Gem, or with L_RD or free Dox at a concentration equivalent to 50 μM Dox. At 3, 6, 12, and 24 h post-treatment, the cells were rinsed twice with cold PBS, trypsinized and collected by centrifugation at 233 rcf. The cell pellets were suspended in PBS and lysed by three cycles of freezing and thawing followed by probe sonication. The protein content in each cell lysate was measured by micro BCA assay. A hundred microliters of cell lysate was mixed with 200 μL of acetonitrile, bath sonicated for 1 h, and centrifuged at 16100 rcf for 30 min to separate a supernatant. The supernatant was evaporated under vacuum overnight and reconstituted in 100 μL of PBS. Dox was detected by the microplate reader at $\lambda_{Ex}/\lambda_{Em}$ of 488 nm/580 nm. dFdCTP was detected by HPLC using a 64:36 v/v mixture of two aqueous mobile phases: (i) KH_2PO_4 10 mM, tetra butyl ammonium bromide (TBABr) 10 mM, pH 7 and 0.25% methanol and (ii) KH_2PO_4 250 mM, TBABr 10 mM, pH 7 and 15% methanol, run at 1.2 mL/min, and a detection wavelength of 271 nm.[31]

2.8.2. Confocal microscopic imaging—Huh7 cells were seeded in a 35 mm glass-bottomed dish (Mat Tek Corp., Ashland, MA) at a density of 100,000 cells per dish. At 70%

confluence, the cells were treated with free Dox for 10 min or fluorescently labeled liposomes (*L_RD, labeled with 25-NBD cholesterol) for 10 min, 3 h or 10 h. At each time point, the cells were rinsed twice with PBS. After nuclei staining with Hoechst 33342 (5 μg/mL) for 10 min, the cells were rinsed again with PBS and imaged in medium by a Nikon-A1R confocal microscope (Nikon America Inc., Melville, NY). For selected treatments, chloroquine was added 12 h prior to the treatment. The cells were rinsed with PBS and incubated with the labeled liposomes for confocal imaging.

2.8.3. Flow cytometry—To supplement the confocal microscopic imaging, flow cytometry was performed with cells treated in the same manner as above. Huh7 cells were seeded in a 48 well-plate at a density of 50,000 per well. After overnight incubation, the cells were treated with free Dox for 10 min or L_RD for 10 min, 3h or 10 h at a concentration equivalent to 50 μM Dox. Cells were then rinsed with PBS and analyzed by an Accuri C6 flow cytometer (BD Biosciences, San Jose, CA) with an FL-2 detector ($\lambda_{ex}/\lambda_{em}$ = 488 nm/585 nm).

2.9. In vivo delivery of liposomal combination

2.9.1. Huh7 xenograft model—All the animal procedures were approved by Purdue Animal Care and Use Committee, in conformity with the NIH guideline for the care and use of laboratory animals. 4–5 week old male athymic nude mice (Foxn1nu) were purchased from Envigo (Indianapolis, IN) and acclimatized for 4 days prior to the procedure. Each mouse received a subcutaneous injection of 10^7 Huh7 cells in the upper flank of the right hind leg. The tumor length (L) and width (W) were measured by a digital caliber, and tumor volume (V) was calculated according to the equation: $V = (L \times W^2)/2$.

2.9.2. Intravenous administration of treatments in Huh7 tumor bearing mice —When the tumor reached 100 mm^3 (~21 days after inoculation), the mice were randomized into 3 groups and treated with a free drug mixture comprising 1.8 mg/kg/dose Gem and 4 mg/kg/dose of Dox (n = 4) or a mixture of their liposomal counterparts at the same doses (n = 4) by tail-vein injection. Eight hours post injection, the mice were sacrificed to sample blood and tumors. Blood was collected in BD Vacutainer containing lithium heparin (BD Biosciences, San Jose, CA) and centrifuged at 4000 rcf to separate plasma.

2.9.3. Sample preparation—For the plasma sample extraction, 20 μL of the sample or calibration standard was transferred to glass tubes, followed by the addition of an internal standard and ethyl acetate. The samples were then vortexed, centrifuged, and the organic layer was transferred to a clean glass tube, and evaporated to dryness. The samples were then reconstituted with mobile phase for HPLC-MS/MS analysis. The tumor sample was weighed and transferred to a glass tube. PBS was added to the sample to bring the total volume to 1 mL. The tissue was then homogenized using a TissueRuptor® with a single use disposable probe. An 0.5 mL aliquot was transferred to a clean glass tube and handled in the same manner as plasma.

2.9.4. Drug analysis—Dox, doxorubicinol (a metabolite of Dox), Gem, and 2',2'-difluorodeoxyuridine (dFdU, a deaminated metabolite of Gem) in each sample were

analyzed by HPLC-MS/MS (Agilent 1290 pump, Eskigent Autosampler, and 5500 QTRAP® Sciex). Temazepam (20 μL of 0.1 ng/μL) was used as an internal standard for Dox and doxorubicinol, and 5-azacytadine (20 μL of 1 ng/μL) for Gem and dFdU. Dox, doxorubicinol, and temazepam were separated on a Phenomenex Monolithic Onyx C18 100 × 4.6 mm column with acetonitrile containing 0.1% formic acid delivered on a gradient at a flow rate of 800 μL/min. Gem, dFdU, and 5-azacytadine were separated on an Agilent Zorbax C8 250 × 4.6 mm 5-micron column with acetonitrile containing 5 mM ammonium formate delivered on a gradient at a flow rate of 800 μL/min. The mass spectrometer utilized an electrospray ionization probe run in positive mode. The multiple reaction monitoring (MRM) Q1/Q3 (m/z) transitions for Dox, doxorubicinol, and temazepam were 544.0/369.9, 546.3/398.9, and 301.0/255.2, respectively. The MRM Q1/Q3 (m/z) transitions for Gem, dFdU, and 5-azacytadine were 264.0/112.1, 265.0/112.8, and 245.0/113.0, respectively. The lower limit of quantification (LOQ) was 3 ng/mL for both Dox and doxorubicinol and 1 ng/mL for both Gem and dFdU.

2.10. Anti-tumor efficacy of liposomal combination

Tumor-bearing mice were prepared in the same way as in 2.9.1. When the tumor volume reached 100 mm^3, the mice were randomized to 3 groups and treated with PBS (n = 6), a free drug mixture comprising 1.8 mg/kg/dose Gem and 4 mg/kg/dose of Dox (n = 8), or a mixture of their liposomal counterparts at the same doses (n = 8) by tail-vein injection. Each treatment was repeated four times with a 7-day interval (q7d × 4). The tumor volume and body weight were monitored daily. The tumor specific growth rate was calculated as $\Delta \log V / \Delta t$ (t: time in days).[32] Animals with tumors reaching more than 10% of the body weight were humanely euthanized.

To examine the effect of each treatment on tumor and major organs, another set of tumor-bearing mice were treated once with PBS (n = 2), a free drug mixture (1.8 mg/kg Gem and 4 mg/kg of Dox) (n = 3), or a mixture of their liposomal counterparts (n = 3) by tail-vein injection. One week after the treatment, animals were humanely sacrificed, and the organs and tumors were collected, fixed in 10% neutral buffered formalin solution, embedded in paraffin, and stained with hematoxylin and eosin for histological evaluation. Unstained paraffin-embedded tumor sections were analyzed by the TUNEL assay for the evaluation of pro-apoptotic effect of the treatment. Three to four randomly selected fields per each TUNEL-stained slide were imaged with a Nikon A1R confocal microscope and analyzed by Nikon A1R image analysis software to count apoptotic cells and nuclei. Percent apoptotic cells were calculated as the ratio of the number of apoptotic cells to the number of nuclei.

2.11. Statistical analysis

All data were expressed as means ± standard deviations. Statistical analyses were performed with GraphPad Prism 7 (San Diego, CA). Data were analyzed by ANOVA test followed by recommended post-hoc multiple comparisons tests. A p value of < 0.05 was considered statistically significant.

3. Results and Discussion

3.1. Effect of preparation methods on liposomal drug loading

Gem-loaded liposomes by passive loading (L_PG) showed a negligible drug loading of 0.14 wt%. However, variations in the drug loading method, such as remote loading, small volume loading, and hypertonic loading, increased the Gem loading capacity to 3.7 wt% (L_RG), 3.8 wt% (L_SG), and 2.4 wt% (L_HG), respectively (Supporting Table 1). With the combination of remote loading and small volume or hypertonic loading (Table 1), the Gem loading capacity further increased to 9.4 ± 0.6 wt% ($L_{RS}G$) and 10.3 ± 1.4 wt% ($L_{RH}G$). Dox-loaded liposomes, made by the remote loading method (L_RD), showed the loading capacity of 21.3 ± 2.5 wt%, which approaches the theoretical Dox content (5/(20 + 5) = 20 wt%), consistent with a previous report.[33]

The remote loading relies on the pH gradient across the lipid bilayer created by the ionization of ammonium sulfate and the diffusion of ammonia, which provides a driving force for the influx of unionized drug. The internalized drug undergoes ionization in the acidic internal pH (3.6[2]) and forms a stable sulfate complex, which is precipitated inside the liposomes.[1] This principle works well for Dox[4] but not for Gem. Due to the low pKa value (3.6), the extent of Gem ionization in the interior of liposomes (ionized/unionized = 1) is not as high as Dox with a pKa value of 8.68 (ionized/unionized = 120,000); therefore, the loading capacity of L_RG (3.7 wt%) was much lower than that of L_RD (21.3 wt%). Of note, our loading capacity of L_RG (3.7 wt%) is substantially higher than that reported by Xu et al (0.2 wt%).[8] This difference may be attributable to the fact that the Gem concentration in the exterior of the liposomes was kept 38 times higher than Xu's (10 mg/mL vs. 0.26 mg/mL), which helped increase the concentration gradient of unionized Gem across the lipid bilayer. This is consistent with the principle of the small volume loading, which employs the maximum concentration gradient to facilitate drug influx into the liposomes.[8] With the small volume loading method, the loading capacity of L_SG was 3.8 wt%, comparable to the previous studies (4 wt%[8]; 4.3 wt%[29]). The hypertonic loading method also helped to enhance the loading capacity of Gem. In this method, liposomes were filled with hypertonic sodium chloride solution (462 mM) and suspended in Gem solution (10 mg/mL: i.e., 38 mM). The difference in ionic strengths created a high osmotic pressure inside the liposomes, pulling Gem along with water into the aqueous core of the liposomes. The combination of remote loading and small volume loading or hypertonic loading further increased the Gem loading. This enhancement demonstrates that the benefit of remote loading can be maximized when combined with additional means to increase the influx of unionized Gem, be it through increasing the concentration gradient (via small volume loading) or the osmotic pressure gradient (via hypertonic loading).

The combination of remote loading and small volume loading was also used to co-encapsulate Dox and Gem ($L_{RS}GD$). The loading contents of Dox and Gem were 10.0 ± 2.1 wt% and 4.2 ± 1.0 wt%, respectively, about half the maximum drug contents of the liposomes loaded with Dox or Gem individually (L_RD; $L_{RS}G$ or $L_{RH}G$) (Table 1). This reduction in drug loading capacity may be explained by the competition between Gem and Dox for available sulfate.

3.2. Particle characterization

The z-averages of liposomes measured by DLS were 210–220 nm (Table 1). The zeta potential measured in 1 mM phosphate buffer (pH 7.4) was consistently negative irrespective of the loaded drug, likely due to the presence of cholesterol that reduces the binding of sodium ions to the membrane surface.[34] DSPE-PEG_{2000} may also have contributed to the negative charge.[35] The particle size and zeta potential of Gem-loaded liposomes ($L_{RS}G$, $L_{RH}G$) did not change significantly over 3-month storage at 4 °C (Table 2). L_RD was also stable for the first 2 months but showed a slight increase in size in the third month. $L_{RS}GD$ showed significant size increase after 1-month storage. Despite variable size stability, the drug contents did not change during the storage indicating stable liposomal encapsulation of the drugs (Table 2).

The particle size of the Gem-loaded liposomes ($L_{RS}G$, $L_{RH}G$) estimated by TEM using ImageJ was consistent with the DLS measurement, which ranged from 152 to 315 nm (Fig. 2). In TEM micrographs, the interior of $L_{RS}G$ and $L_{RH}G$ appeared darker than blank counterparts, with many of them showing a triangular shape, which is likely the Gem sulfate complex. L_RD liposomes were filled with rod-shape precipitates (data not shown), typical of Dox sulfate complexes.[36]

3.3. In vitro release kinetics of liposomal drugs

The drug release from liposomes were examined in phosphate-buffered saline (phosphate 10 mM) at pH 7.4 and pH 5.5, representing extracellular and lysosomal pHs, respectively (Fig. 3). Both $L_{RS}G$ and $L_{RH}G$ showed a sustained Gem release, irrespective of the pH (except for the initial delay with $L_{RS}G$ at pH 7.4), with ~60% of the encapsulated Gem released by 120 h. Given the contrast with L_PG (passive loading with no sulfate complex), which released ~100% of drug in 5 h, the sustained release profiles of $L_{RS}G$ and $L_{RH}G$ may be attributable to the formation of Gem sulfate complex, which does not readily pass the lipid bilayer.[9, 14] L_RD also showed a sustained release profile with a similar mechanism, but the extent of Dox release was pH-dependent (40% at pH 7.4 and 60% at pH 5.5 by 120 h). The pH-dependent Dox release from liposomal Dox has been reported in the literature.[3, 37] The increased Dox release at acidic medium is likely driven by the influx of protons, which causes the dissociation (dissolution) of Dox sulfate (Supporting Fig. 1b). The extent of pH-dependence in drug release is shown to vary with the type of counterions, which determines their tendency of protonation, hence the dissolution of ionic Dox complex.[3] The acidic pH would not have affected Gem release as much as it did Dox, as a relatively large fraction of Gem would be present in the free base form due to the low pKa value.

$L_{RS}GD$ showed different drug release patterns (Supporting Fig. 2), indicating the influence of one drug on the other. Gem release from the $L_{RS}GD$ showed pH-dependence, with 71% released at pH 7.4 and 82% at pH 5.5 by 120 h. This suggests that Dox and Gem have shared sulfate to form a co-complex (i.e., Dox-sulfate-Gem) and the dissolution of Dox sulfate at acidic pH induced concomitant dissociation of Gem. Dox release from the $L_{RS}GD$ continued to be pH-dependent but was overall suppressed by 20%, likely due to the competition with Gem in the co-complex. $L_{RS}GD$ was excluded in the following studies, since it had no

outstanding advantages in drug loading capacity and storage stability but confounding interactions between the drugs in controlled release.

3.4. Cytotoxicity of liposomal drugs vs. free drug counterparts

$L_{RS}G$, $L_{RH}G$ and L_RD incubated with Huh7 cells for 72 h showed similar cytotoxicity as free drug counterparts (Fig. 4) with comparable IC_{50} values (1.6 μM, 4.3 μM, 3.0 μM for free Gem, $L_{RS}G$, and $L_{RH}G$; 0.25 μM and 0.32 μM for free Dox and L_RD). Blank liposomes did not show significant cytotoxicity (Supporting Fig. 3). This result indicates that the liposomes released active drugs during the incubation.

In another setting, the cells were exposed to the liposomes for a short time period (6 h for Gem; 3 h for Dox) to simulate dynamic in vivo environment, where the contact between the treatment and tumor cells declines with time. The cell viability after short-term exposure treatment reflects the effect of drug (as the released drug or liposomal drug) taken up by the cells during the exposure. With 6 h incubation, $L_{RS}G$ and $L_{RH}G$ showed greater toxicity than the equivalent dose of free Gem, reaching a statistical difference at 100 μM (Fig. 5a). Given that Gem release from the liposomes in the first 6 h was <20%, the greater toxicity of liposomal Gem may mainly be attributable to the improvement in cellular uptake of the drug, which is necessary to its intracellular conversion to bioactive metabolite (dFdCTP).[7] Free Gem is known to enter cells poorly due to the high hydrophilicity[38] and the dependence on nucleoside transporters.[39–41] Liposomal Gem may be more efficient than free Gem as they can enter cells[42] by diverse endocytic pathways.[43] In contrast, L_RD showed less toxicity than free Dox after 3 h exposure (significant difference shown at a concentration equivalent to Dox 1 μM, Fig. 5b), consistent with relatively slow Dox release. This suggests that liposomal Dox does not have advantage over free Dox as liposomal Gem does over free Gem in the cell level.

3.5. Cellular uptake of liposomal drugs vs. free drug counterparts

To verify whether liposomal Gem enters cells more efficiently than free Gem (and liposomal Dox does the opposite), cellular uptake of each liposomes was investigated by measuring intracellular drug contents after timed incubation. As expected, Huh7 cells incubated with $L_{RS}G$ or $L_{RH}G$ showed greater intracellular concentration of dFdCTP than those treated with free Gem (statistical difference shown at 6 and 12 h incubation, Fig. 5c). This result supports that the liposomal Gem improves the activity of Gem by increasing its intracellular delivery. L_RD vs. free Dox showed the opposite trend, with free Dox entering cells more efficiently than L_RD, as evident at 3, 6, and 12 h (Fig. 5d). The attenuated cellular uptake relative to free Dox coupled with slow drug release (Fig. 3b) may account for the relatively low activity of L_RD after 3 h exposure (Fig. 5b).

Confocal microscope imaging further confirmed the delayed cellular uptake and drug release of L_RD. Free Dox entered the cells more quickly than $*L_RD$ (L_RD labeled with 25-NBD cholesterol), appearing in the nuclei as early as in 10 min (Fig. 6a). Flow cytometry confirmed that Dox fluorescence intensity of free Dox-treated cells was stronger than that of the L_RD-treated cells after 10 min incubation (Supporting Fig. 4a). While the fluorescent cholesterol signal was observed in the cells in 10 min indicating the uptake of liposomes,

Dox signal took longer to show up in the cells. The time-dependent increase of Dox signal in L_RD-treated cells was observed by flow cytometry (Supporting Fig. 4b). When Dox was detected in the L_RD-treated cells (at 3 h and 10 h), part of the signal was present in the cytosol in addition to the nucleus, reflecting the fraction of Dox remaining in the liposomes (Fig. 6b). When the cells were pretreated with chloroquine (CQ), which prevents the acidification of the lysosomes by consuming protons,[44–46] Dox fluorescence appeared as punctate signals in the cytosol with little signal in the nuclei. This indicates that $*L_RD$ was taken up by endocytosis and trafficked to lysosomes and Dox release was delayed in the CQ-filled (hence less acidic) lysosomes, consistent with the acid-dependent release kinetics of liposomal Dox (Fig. 3b).

3.6. Optimization of Dox/Gem combination

The bioactivity of liposomal Gem was tested in the context of combination therapy with Dox. To determine the optimal regimen for Gem/Dox combination treatment, free drug combinations were first tested with Huh7 cells in different sequences and ratios, keeping the exposure to each drug to 1 day. Simultaneous treatment (Gem + Dox) yielded relatively low CI values compared to sequential treatments at all ratios (Fig. 7a, Table 3). Accordingly, Huh7 cells were treated with combinations of liposomes simultaneously ($L_{RS}G + L_RD$ or $L_{RH}G + L_RD$). The liposomal mixtures were found to be synergistic at all tested ratios (Fig. 7b, Table 4), when measured after 3 d exposure. For the following in vivo study, $L_{RS}G + L_RD$ combination at 1:1 molar ratio was selected to avoid using one drug in a disproportionately high dose to exceed its maximum tolerated dose.

3.7. In vivo delivery of liposomal combination

Huh7 tumor bearing mice were administered intravenously with 1:1 molar combination of $L_{RS}G + L_RD$ or free drug mixture to compare their in vivo delivery. Animals were sacrificed at 8 h post-treatment, and the concentrations of each drug and its metabolite in plasma and tumor measured (Supporting Figs. 5 and 6). The samples from animals treated with the liposomal combination ($L_{RS}G + L_RD$) showed significant levels of Gem and Dox in either the original or metabolite form (Fig. 8). In contrast, the drugs were undetectable in the samples of free drug mixture-treated group. This difference between liposomal and free drug mixtures is consistent with the extended circulation time of PEGylated liposomes.[47–49] Notably, most Gem in tumors of the liposomal combination group was detected in the metabolized form (dFdU). This indicates that $L_{RS}G$ arriving at tumors was taken up by the cells and underwent intracellular metabolism, in accordance with in vitro cellular uptake of liposomal Gem's (Fig. 5c). Nevertheless, it is noted that this measurement was performed at a single time point (8 h) after the treatment. Pharmacokinetics and biodistribution studies remain to be performed in order to fully evaluate the contribution of the liposomal formulation to in vivo delivery of Gem.

3.8. Anti-tumor efficacy of liposomal combination

$L_{RS}G + L_RD$ combination was simultaneously administered to male nude mice inoculated with subcutaneous Huh7 tumors at a q7d × 4 schedule and compared with those treated with free drug combination at the equivalent dose (Fig. 9a). The total administered dose (1.8 mg/kg/dose Gem and 4 mg/kg/dose of Dox, q7d × 4) was below the reported maximum

tolerated dose of each drug (16 mg/kg for Gem[50]; 30 mg/kg for Dox[51]). Both free drug and liposomal combinations were well tolerated without causing >20% weight loss during the treatment (Supporting Fig. 7) and induced significant delay in tumor growth as compared to PBS (free drug combination: $p < 0.01$; liposomal combination: $p < 0.001$ vs. PBS group, by Tukey's test) (Fig. 9b, c). The animals treated with the liposomal combination showed a significant extension in the median survival time compared with the PBS or free drug combination-treated animals (Fig. 9d; $p < 0.0001$ vs. PBS group; $p < 0.001$ vs. free drug combination group by Log-rank (Mantel-Cox) test). Although the drug levels in tumors (Fig. 8) suggest that both $L_{RS}G$ and L_RD have played roles in the enhanced anti-tumor efficacy, the relative contribution of each liposomal drug to the effect may not be ascertained without comparison with the monotherapy based on single liposome treatment.

The effects of each treatment on tumor and other major organs that may be affected by free drug (heart, liver or kidney)[52,53] were examined at 7 days after single treatment, by TUNEL assay and histological evaluation. In TUNEL assay, the tumor sections of $L_{RS}G+L_RD$-treated animals showed higher numbers of apoptotic cells than those of the PBS-treated animals, consistent with the specific tumor growth rate, whereas those treated with free drug combination showed no significant difference from the control group at this time point (Fig. 10a; Supporting Fig. 8). Histological evaluation showed a consistent trend, indicating a greater population of dying cells in $L_{RS}G+L_RD$-treated tumors (Fig. 10b; Supporting Fig. 9). The PBS-treated animals showed highly vascular tumors, where tumor cells were arranged in sheets with cellular and nuclear pleomorphism with abnormal nuclear morphology. Fifty-seven mitotic figures were identified in ten 40× fields. In the tumors of animals treated with free drug combination, cellular morphology was similar to that of the control. Occasional cells were necrotic with hypereosinophilic cytoplasm and karryorhexis. On the other hand, tumors of animals treated with $L_{RS}G+L_RD$ were composed of neoplastic cells arranged in sheets and contained multifocal areas of cellular necrosis. Necrotic tumor cells had a hypereosinophilic cytoplasm with shrunken nuclei, and these cells were surrounded by erythrocytes and mixed inflammatory cell population. Differential toxicity on off-target organs between free drug combination- and $L_{RS}G+L_RD$-treated animals was suspected based on the literature supporting the benefit of liposomal drug[54–59] but not observed at the dose (one time treatment of 1.8 mg/kg Gem and 4 mg/kg of Dox) and time point (7 days after treatment) used in this study, with neither group showing abnormality in those organs compared to the PBS-treated group.

4. Conclusion

Liposomal Gem with high drug loading capacity was produced by remote loading, small volume loading, hypertonic loading, and their combinations. Each method increased the loading capacity from 0.14 wt% to 3.7 wt% (remote loading), 3.8 wt% (small volume loading), and 2.7 wt% (hypertonic loading), respectively. The combination of remote loading and small volume loading or hypertonic loading further increased the Gem loading capacity to 9.4 ± 0.6 wt% and 10.3 ± 1.4 wt%, respectively, based on the increased influx and efficient entrapment of Gem in the liposomal core. The liposomal Gem showed high stability, sustained drug release, enhanced cellular uptake, and improved cytotoxicity as compared to free Gem. Liposomal Gem showed a synergistic effect with liposomal Dox on

Huh7 hepatocellular carcinoma cells. A mixture of liposomal Gem and liposomal Dox delivered both drugs to the tumor more efficiently than a free drug mixture and showed a relatively good anti-tumor effect in a xenograft model of Huh7 tumor. This study demonstrates the feasibility of producing bioactive liposomal Gem with an unprecedented high drug loading capacity.

Supplementary Material

Refer to Web version on PubMed Central for supplementary material.

Acknowledgments

This work was supported by NIH R01 EB017791, NIH R01 CA232419 and the Fellowship support from the Egyptian Government Ministry of Higher Education Missions Sector to H.T. The authors thank Prof. Wanqing Liu of Wayne State University for kind donation of Huh7 cells and Prof. Wooin Lee of Seoul National University for discussion of in vivo drug delivery. Drug concentrations in plasma and tumors were analyzed by the Clinical Pharmacology Analytical Core laboratory, a core laboratory of the Indiana University Melvin and Bren Simon Cancer Center supported by the National Cancer Institute grant P30 CA082709.

References

1. Haran G; Cohen R; Bar LK and Barenholz Y, Transmembrane ammonium sulfate gradients in liposomes produce efficient and stable entrapment of amphipathic weak bases. Biochimica et Biophysica Acta (BBA) - Biomembranes 1993, 1151, 201–215. [PubMed: 8373796]
2. Gubernator J, Active methods of drug loading into liposomes: recent strategies for stable drug entrapment and increasedin vivoactivity. Expert Opinion on Drug Delivery 2011, 8, 565–580. [PubMed: 21492058]
3. Fritze A; Hens F; Kimpfler A; Schubert R and Peschka-Suss R, Remote loading of doxorubicin into liposomes driven by a transmembrane phosphate gradient. Biochim Biophys Acta 2006, 1758, 1633–40. [PubMed: 16887094]
4. Barenholz Y, Doxil$^{(R)}$--the first FDA-approved nano-drug: lessons learned. J Control Release 2012, 160, 117–34. [PubMed: 22484195]
5. Barenholz Y, Liposome application: problems and prospects. Current Opinion in Colloid & Interface Science 2001, 6, 66–77.
6. Gabizon A; Catane R; Uziely B; Kaufman B; Safra T; Cohen R; Martin F; Huang A and Barenholz Y, Prolonged Circulation Time and Enhanced Accumulation in Malignant Exudates of Doxorubicin Encapsulated in Polyethylene-glycol Coated Liposomes. Cancer Res 1994, 54, 987–992. [PubMed: 8313389]
7. de Sousa Cavalcante L and Monteiro G, Gemcitabine: metabolism and molecular mechanisms of action, sensitivity and chemoresistance in pancreatic cancer. Eur J Pharmacol 2014, 741, 8–16. [PubMed: 25084222]
8. Xu H; Paxton J; Lim J; Li Y; Zhang W; Duxfield L and Wu Z, Development of high-content gemcitabine PEGylated liposomes and their cytotoxicity on drug-resistant pancreatic tumour cells. Pharm Res 2014, 31, 2583–92. [PubMed: 24639234]
9. Celano M; Calvagno MG; Bulotta S; Paolino D; Arturi F; Rotiroti D; Filetti S; Fresta M and Russo D, Cytotoxic effects of gemcitabine-loaded liposomes in human anaplastic thyroid carcinoma cells. BMC Cancer 2004, 4, 63. [PubMed: 15363094]
10. Yeo Y and Kim B-K, Drug Carriers: Not an Innocent Delivery Man. AAPS J. 2015, 17, 1096–1104. [PubMed: 26017163]
11. Ernsting MJ; Murakami M; Undzys E; Aman A; Press B and Li S-D, A Docetaxel-Carboxymethylcellulose Nanoparticle Outperforms the Approved Taxane Nanoformulation, Abraxane, in Mouse Tumor Models with Significant Control of Metastases. J. Control. Release 2012, 162, 575–581. [PubMed: 22967490]

12. Wilhelm S; Tavares AJ; Dai Q; Ohta S; Audet J; Dvorak HF and Chan WCW, Analysis of Nanoparticle Delivery to Tumours. Nat. Rev. Mater 2016, 1, 16014.
13. Mayer LD; Tai LCL; Ko DSC; Masin D; Ginsberg RS; Cullis PR and Bally MB, Influence of Vesicle Size, Lipid Composition, and Drug-to-Lipid Ratio on the Biological Activity of Liposomal Doxorubicin in Mice. Cancer Res 1989, 49, 5922. [PubMed: 2790807]
14. Federico C; Morittu VM; Britti D; Trapasso E and Cosco D, Gemcitabine-loaded liposomes: rationale, potentialities and future perspectives. Int J Nanomedicine 2012, 7, 5423–36. [PubMed: 23139626]
15. Dasanu CA, Gemcitabine: Vascular Toxicity and Prothrombotic Potential. Expert Opin. Drug Saf 2008, 7, 703–716. [PubMed: 18983217]
16. Rivera E; Valero V; Arun B; Royce M; Adinin R; Hoelzer K; Walters R; Wade JL; Pusztai L and Hortobagyi GN, Phase II Study of Pegylated Liposomal Doxorubicin in Combination With Gemcitabine in Patients With Metastatic Breast Cancer. Journal of Clinical Oncology 2003, 21, 3249–3254. [PubMed: 12947059]
17. Pérez-Manga G; Lluch A; Alba E; Moreno-Nogueira JA; Palomero M; García-Conde J; Khayat D and Rivelles N, Gemcitabine in Combination With Doxorubicin in Advanced Breast Cancer: Final Results of a Phase II Pharmacokinetic Trial. Journal of Clinical Oncology 2000, 18, 2545–2552. [PubMed: 10893285]
18. Yang TS, Gemcitabine and doxorubicin for the treatment of patients with advanced hepatocellular carcinoma: a phase I-II trial. Annals of Oncology 2002, 13, 1771–1778. [PubMed: 12419750]
19. Lombardi G; Zustovich F; Farinati F; Cillo U; Vitale A; Zanus G; Donach M; Farina M; Zovato S and Pastorelli D, Pegylated liposomal doxorubicin and gemcitabine in patients with advanced hepatocellular carcinoma: results of a phase 2 study. Cancer 2011, 117, 125–33. [PubMed: 21058409]
20. Nahire R; Haldar MK; Paul S; Ambre AH; Meghnani V; Layek B; Katti KS; Gange KN; Singh J; Sarkar K and Mallik S, Multifunctional polymersomes for cytosolic delivery of gemcitabine and doxorubicin to cancer cells. Biomaterials 2014, 35, 6482–6497. [PubMed: 24797878]
21. Anajafi T; Scott MD; You S; Yang X; Choi Y; Qian SY and Mallik S, Acridine Orange Conjugated Polymersomes for Simultaneous Nuclear Delivery of Gemcitabine and Doxorubicin to Pancreatic Cancer Cells. Bioconjugate Chemistry 2016, 27, 762–771. [PubMed: 26848507]
22. Vogus DR; Evans MA; Pusuluri A; Barajas A; Zhang M; Krishnan V; Nowak M; Menegatti S; Helgeson ME; Squires TM and Mitragotri S, A hyaluronic acid conjugate engineered to synergistically and sequentially deliver gemcitabine and doxorubicin to treat triple negative breast cancer. J Control Release 2017, 267, 191–202. [PubMed: 28823957]
23. Vogus DR; Pusuluri A; Chen R and Mitragotri S, Schedule dependent synergy of gemcitabine and doxorubicin: Improvement of in vitro efficacy and lack of in vitro-in vivo correlation. Bioeng Transl Med 2018, 3, 49–57. [PubMed: 29376133]
24. Lammers T; Subr V; Ulbrich K; Peschke P; Huber PE; Hennink WE and Storm G, Simultaneous delivery of doxorubicin and gemcitabine to tumors in vivo using prototypic polymeric drug carriers. Biomaterials 2009, 30, 3466–75. [PubMed: 19304320]
25. Liu D; Chen Y; Feng X; Deng M; Xie G; Wang J; Zhang L; Liu Q and Yuan P, Micellar nanoparticles loaded with gemcitabine and doxorubicin showed synergistic effect. Colloids Surf B Biointerfaces 2014, 113, 158–68. [PubMed: 24077114]
26. Immordino ML; Brusa P; Rocco F; Arpicco S; Ceruti M and Cattel L, Preparation, Characterization, Cytotoxicity and Pharmacokinetics of Liposomes Containing Lipophilic Gemcitabine Prodrugs. J. Control. Release 2004, 100, 331–346. [PubMed: 15567500]
27. Modi S; Xiang TX and Anderson BD, Enhanced active liposomal loading of a poorly soluble ionizable drug using supersaturated drug solutions. J Control Release 2012, 162, 330–9. [PubMed: 22800581]
28. Dreis S; Rothweiler F; Michaelis M; Cinatl J Jr.; Kreuter J and Langer K, Preparation, characterisation and maintenance of drug efficacy of doxorubicin-loaded human serum albumin (HSA) nanoparticles. Int J Pharm 2007, 341, 207–14. [PubMed: 17478065]
29. Liu Y; Tamam H and Yeo Y, Mixed Liposome Approach for Ratiometric and Sequential Delivery of Paclitaxel and Gemcitabine. AAPS PharmSciTech 2018, 19, 693–699. [PubMed: 28971370]

30. Chou TC, Theoretical basis, experimental design, and computerized simulation of synergism and antagonism in drug combination studies. Pharmacol Rev 2006, 58, 621–81. [PubMed: 16968952]
31. Losa R; Sierra MI; Gion MO; Esteban E and Buesa JM, Simultaneous determination of gemcitabine di- and triphosphate in human blood mononuclear and cancer cells by RP-HPLC and UV detection. J Chromatogr B Analyt Technol Biomed Life Sci 2006, 840, 44–9.
32. Mehrara E; Forssell-Aronsson E; Ahlman H and Bernhardt P, Specific growth rate versus doubling time for quantitative characterization of tumor growth rate. Cancer Res 2007, 67, 3970–5. [PubMed: 17440113]
33. Niu G; Cogburn B; Hughes J, Preparation and Characterization of Doxorubicin Liposomes, In Cancer Nanotechnology: Methods and Protocols, Grobmyer SR, and Moudgil BM, Editors. Humana Press: Totowa, NJ., 2010, pp. 211–219.
34. Magarkar A; Dhawan V; Kallinteri P; Viitala T; Elmowafy M; Rog T and Bunker A, Cholesterol Level Affects Surface Charge of Lipid Membranes in Saline Solution. Sci. Rep 2014, 4, 5005. [PubMed: 24845659]
35. Webb MS; Saxon D; Wong FMP; Lim HJ; Wang Z; Bally MB; Choi LSL; Cullis PR and Mayer LD, Comparison of Different Hydrophobic Anchors Conjugated to Poly(ethylene glycol): Effects on the Pharmacokinetics of Liposomal Vincristine. Biochim. Biophys. Acta 1998, 1372, 272–282. [PubMed: 9675310]
36. Wei X; Shamrakov D; Nudelman S; Peretz-Damari S; Nativ-Roth E; Regev O and Barenholz Y, Cardinal Role of Intraliposome Doxorubicin-Sulfate Nanorod Crystal in Doxil Properties and Performance. ACS Omega 2018, 3, 2508–2517. [PubMed: 30023837]
37. Shibata H; Izutsu K; Yomota C; Okuda H and Goda Y, Investigation of factors affecting in vitro doxorubicin release from PEGylated liposomal doxorubicin for the development of in vitro release testing conditions. Drug Dev Ind Pharm 2015, 41, 1376–86. [PubMed: 25170659]
38. Zakeri-Milani P; Mussa Farkhani S; Shirani A; Mohammadi S; Shahbazi Mojarrad J; Akbari J and Valizadeh H, Cellular uptake and anti-tumor activity of gemcitabine conjugated with new amphiphilic cell penetrating peptides. EXCLI J 2017, 16, 650–662. [PubMed: 28694765]
39. Lostao MP; Mata JF; Larrayoz IM; Inzillo SM; Casado FJ and Pastor-Anglada M, Electrogenic uptake of nucleosides and nucleoside-derived drugs by the human nucleoside transporter 1 (hCNT1) expressed in Xenopus laevis oocytes. FEBS Letters 2000, 481, 137–140. [PubMed: 10996312]
40. Ueno H; Kiyosawa K and Kaniwa N, Pharmacogenomics of gemcitabine: can genetic studies lead to tailor-made therapy? Br J Cancer 2007, 97, 145. [PubMed: 17595663]
41. Hilbig A and Oettle H, Gemcitabine in the treatment of metastatic pancreatic cancer. Expert Review of Anticancer Therapy 2008, 8, 511–523. [PubMed: 18402518]
42. Celia C; Malara N; Terracciano R; Cosco D; Paolino D; Fresta M and Savino R, Liposomal delivery improves the growth-inhibitory and apoptotic activity of low doses of gemcitabine in multiple myeloma cancer cells. Nanomedicine 2008, 4, 155–166. [PubMed: 18430611]
43. Kang JH; Jang WY and Ko YT, The Effect of Surface Charges on the Cellular Uptake of Liposomes Investigated by Live Cell Imaging. Pharm. Res 2017, 34, 704–717. [PubMed: 28078484]
44. Solomon VR and Lee H, Chloroquine and its analogs: A new promise of an old drug for effective and safe cancer therapies. Eur J Pharmacol 2009, 625, 220–233. [PubMed: 19836374]
45. Steinman M; Mellman S; Muller A and Cohn A, Endocytosis and the Recycling of Plasma Membrane. Journal of cell biology 1983, 96
46. Homewood CA; Warhurst DC; Peters W and Baggaley VC, Lysosomes, pH and the Anti-malarial Action of Chloroquine. Nature 1972, 235, 50. [PubMed: 4550396]
47. Working PK; Newman MS; Huang SK; Mayhew E; Vaage J and Lasic DD, Pharmacokinetics, Biodistribution and Therapeutic Efficacy of Doxorubicin Encapsulated in Stealth® Liposomes (Doxil®). J. Liposome Res 1994, 4, 667–687.
48. Ngoune R; Peters A; von Elverfeldt D; Winkler K and Pütz G, Accumulating Nanoparticles by EPR: A Route of no Return. J. Control. Release 2016, 238, 58–70. [PubMed: 27448444]
49. Torchilin VP, Recent advances with liposomes as pharmaceutical carriers. Nature Reviews Drug Discovery 2005, 4, 145. [PubMed: 15688077]

50. Bornmann C; Graeser R; Esser N; Ziroli V; Jantscheff P; Keck T; Unger C; Hopt UT; Adam U; Schaechtele C; Massing U and von Dobschuetz E, A new liposomal formulation of Gemcitabine is active in an orthotopic mouse model of pancreatic cancer accessible to bioluminescence imaging. Cancer Chemother Pharmacol 2008, 61, 395–405. [PubMed: 17554540]
51. Gallo D; Fruscella E; Ferlini C; Apollonio P; Mancuso S and Scambia G, Preclinical in Vivo Activity of a Combination Gemcitabine/Liposomal Doxorubicin against Cisplatin-Resistant Human Ovarian Cancer (A2780/CDDP). Int J Gynecol Cancer 2006, 16 222–230. [PubMed: 16445637]
52. Chatterjee K; Zhang J; Honbo N and Karliner JS, Doxorubicin cardiomyopathy. Cardiology 2010, 115, 155–162. [PubMed: 20016174]
53. Superfin D; Iannucci AA and Davies AM, Commentary: Oncologic Drugs in Patients with Organ Dysfunction: A Summary. The Oncologist 2007, 12, 1070–1083. [PubMed: 17914077]
54. Gabizon A; Dagan A; Goren D; Barenholz Y and Fuks Z, Liposomes as in Vivo Carriers of Adriamycin: Reduced Cardiac Uptake and Preserved Antitumor Activity in Mice. Cancer Research 1982, 42, 4734–4739. [PubMed: 7127308]
55. Safra T; Muggia F; Jeffers S; Tsao-Wei DD; Groshen S; Lyass O; Henderson R; Berry G and Gabizon A, Pegylated Liposomal Doxorubicin (Doxil): Reduced Clinical Cardiotoxicity in Patients Reaching or Exceeding Cumulative Doses of 500 mg/m2. Annals of Oncology 2000, 11, 1029–1033. [PubMed: 11038041]
56. Gabizon A; Shmeeda H and Barenholz Y, Pharmacokinetics of Pegylated Liposomal Doxorubicin. Clinical Pharmacokinetics 2003, 42, 419–436. [PubMed: 12739982]
57. Rafiyath SM; Rasul M; Lee B; Wei G; Lamba G and Liu D, Comparison of Safety and Toxicity of Liposomal Doxorubicin vs. Conventional Anthracyclines: a Meta-analysis. Experimental hematology & oncology 2012, 1, 10–10. [PubMed: 23210520]
58. O'Brien MER; Wigler N; Inbar M; Rosso R; Grischke E; Santoro A; Catane R; Kieback DG; Tomczak P; Ackland SP; Orlandi F; Mellars L; Alland L and Tendler C, Reduced Cardiotoxicity and Comparable Efficacy in a Phase III trial of Pegylated Liposomal Doxorubicin HCl (CAELYX™/Doxil®) Versus Conventional Doxorubicin for First-Line Treatment of Metastatic Breast Cancer. Annals of Oncology 2004, 15, 440–449. [PubMed: 14998846]
59. Franco YL; Vaidya TR and Ait-Oudhia S, Anticancer and Cardio-Protective Effects of Liposomal Doxorubicin in the Treatment of Breast Cancer. Breast cancer (Dove Medical Press) 2018, 10, 131–141. [PubMed: 30237735]

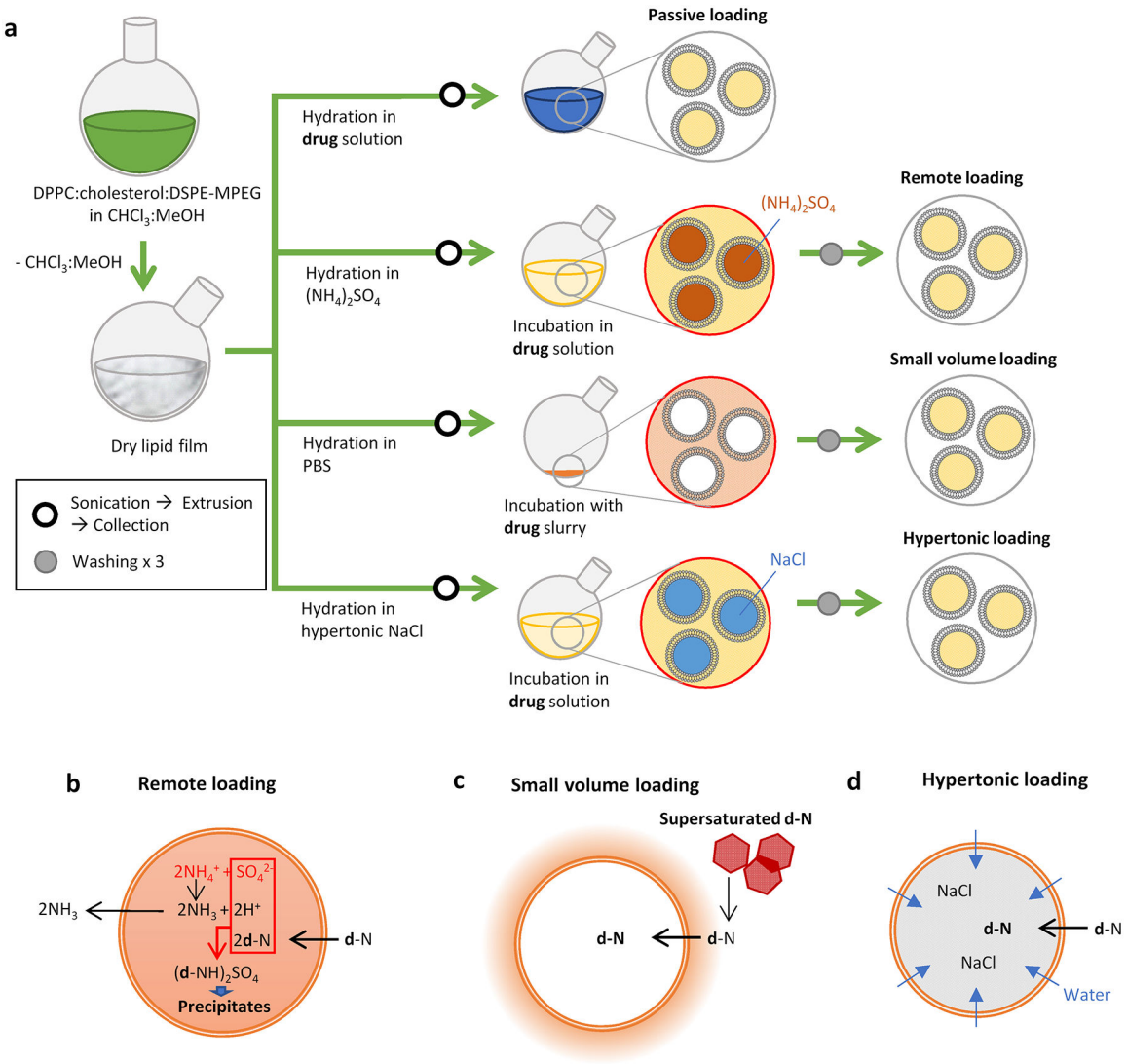

Fig. 1.

Schematic description of the liposome preparation. (a) Overview of passive loading, remote loading, small volume loading, and hypertonic loading. (b-d) Envisioned mechanism of each method. d-N represents weak base drug such as Gem or Dox.

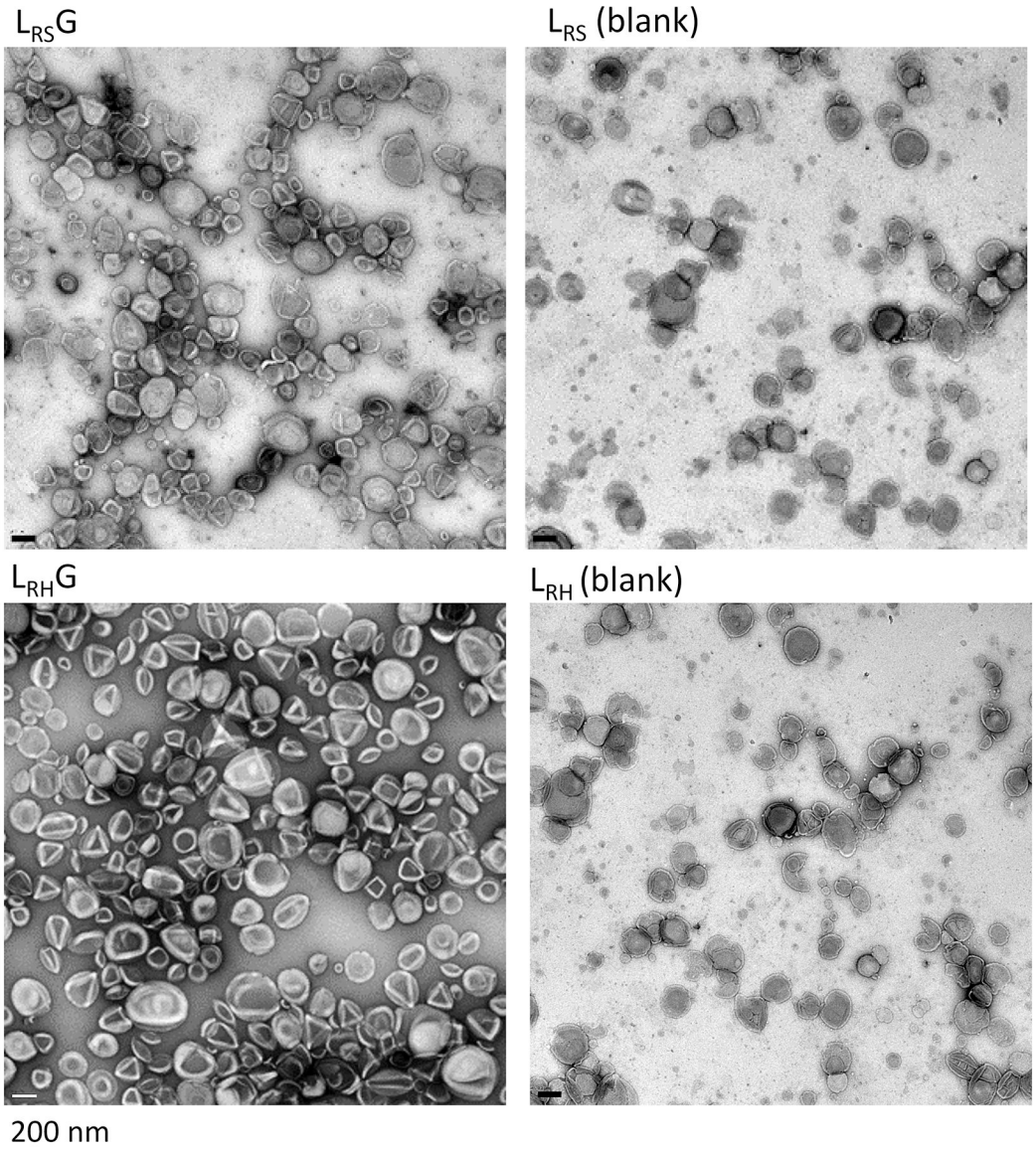

Fig. 2.

TEM images of $L_{RS}G$, $L_{RH}G$, blank L_{RH}, and blank L_{RS}. Scale bar: 200 nm.

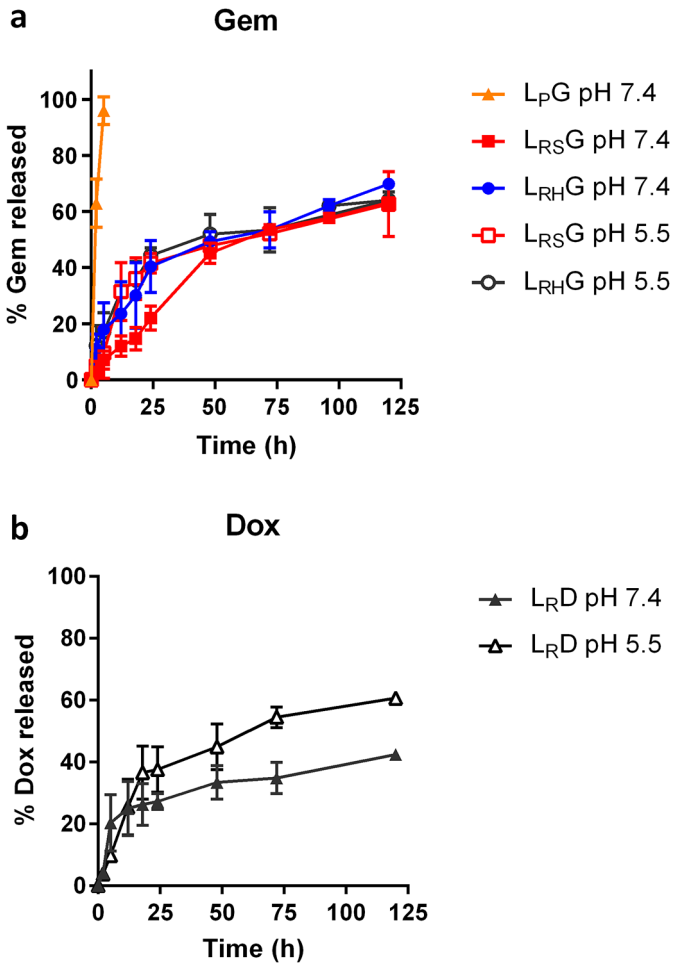

Fig. 3.

In vitro release kinetics of (a) $L_{RS}G$, $L_{RH}G$ and (b) L_RD at pH 5.5 and 7.4. n = 3 independent and identical batches. Mean ± standard deviation (s.d.).

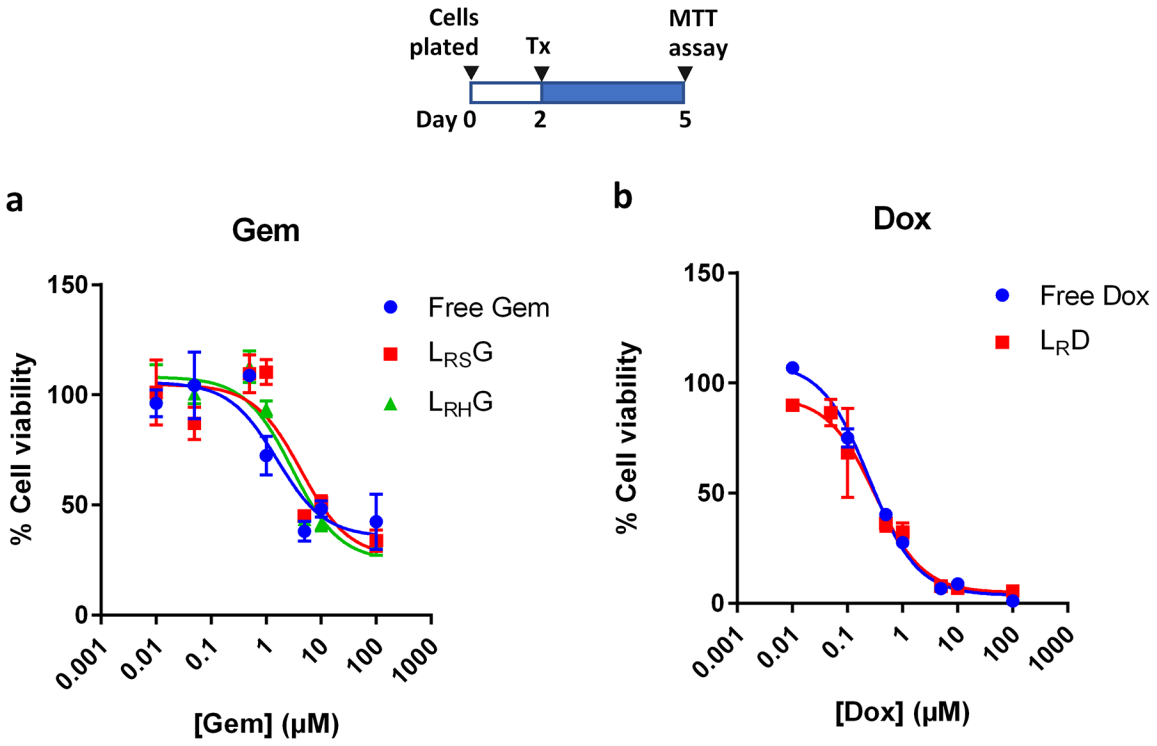

Fig. 4.

Cytotoxicity of (a) free Gem, $L_{RS}G$, and $L_{RH}G$ and (b) free Dox and L_RD after 72 h incubation. n = 3 identical and independent tests. Mean ± s.d.

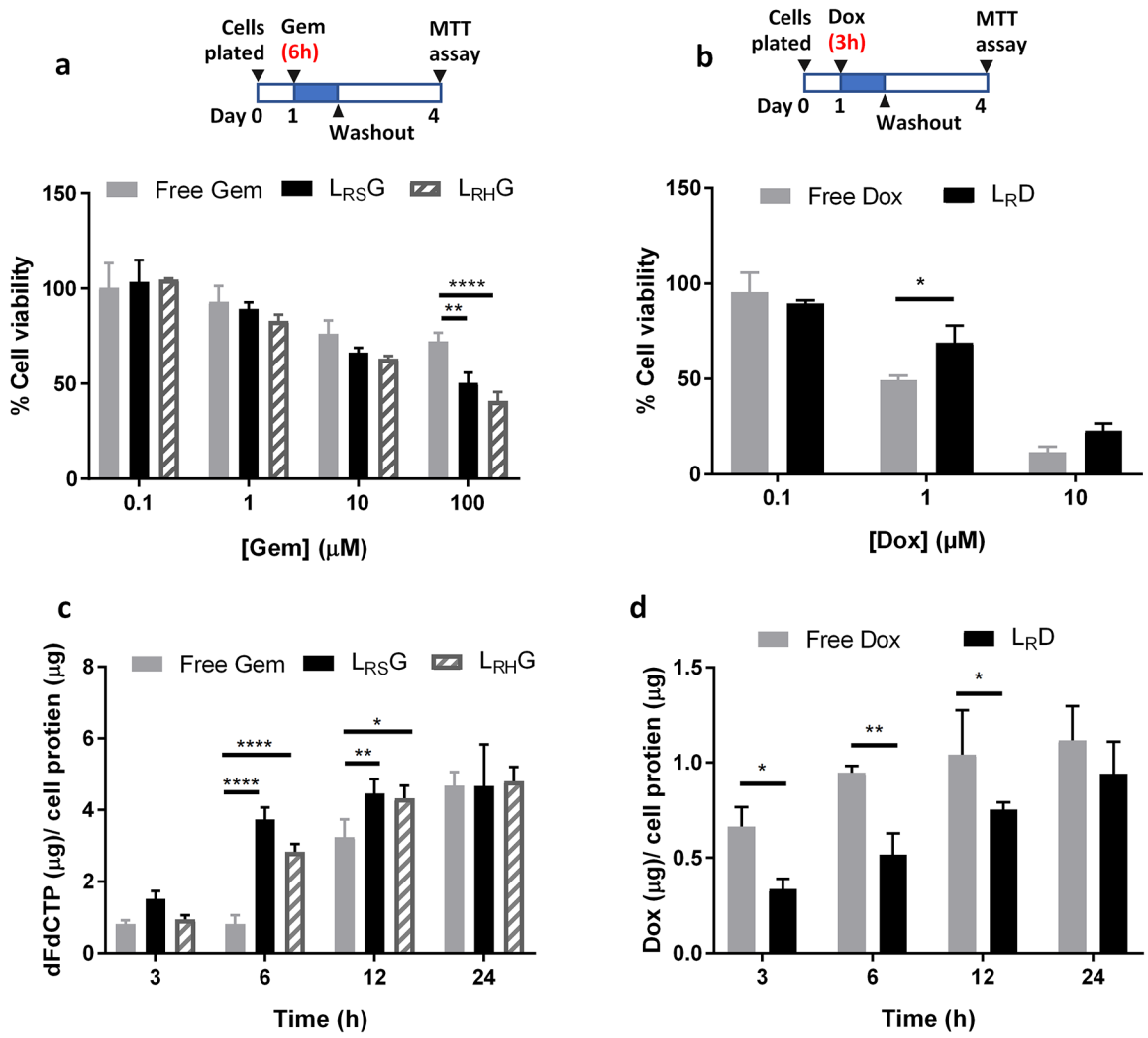

Fig. 5.

Cytotoxicity of (a) free Gem, $L_{RS}G$, and $L_{RH}G$ and (b) free Dox and L_RD after short-term incubation. n = 5 tests of a representative batch. Mean ± s.d. Drug uptake by Huh7 after 3, 6, 12 and 24 h incubation with (c) free Gem, $L_{RS}G$, and $L_{RH}G$ and (d) free Dox and L_RD. n = 3 (Gem) and 4 (Dox) independent and identical tests of a representative batch. Mean ± s.d. *: $p < 0.05$, **: $p < 0.01$ by, ****: $p < 0.0001$ by two-way ANOVA test followed by Sidak's multiple comparisons test.

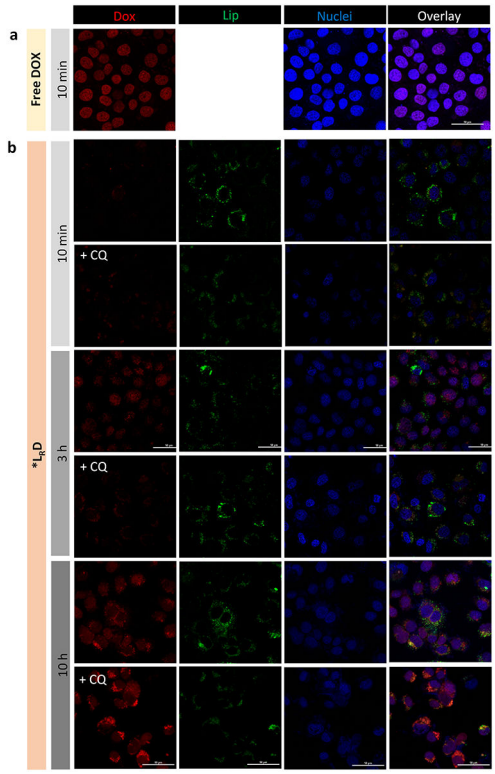

Fig. 6.

Confocal microscopic images of Huh7 cells incubated with (a) free Dox or (b) 25-NBD cholesterol labeled *L_RD for 10 min, 3 h or 10 h. + CQ: cells incubated with chloroquine (inhibitor of endosomal acidification) for 12 h prior to the addition of liposomal Dox. Scale bars: 50 μm.

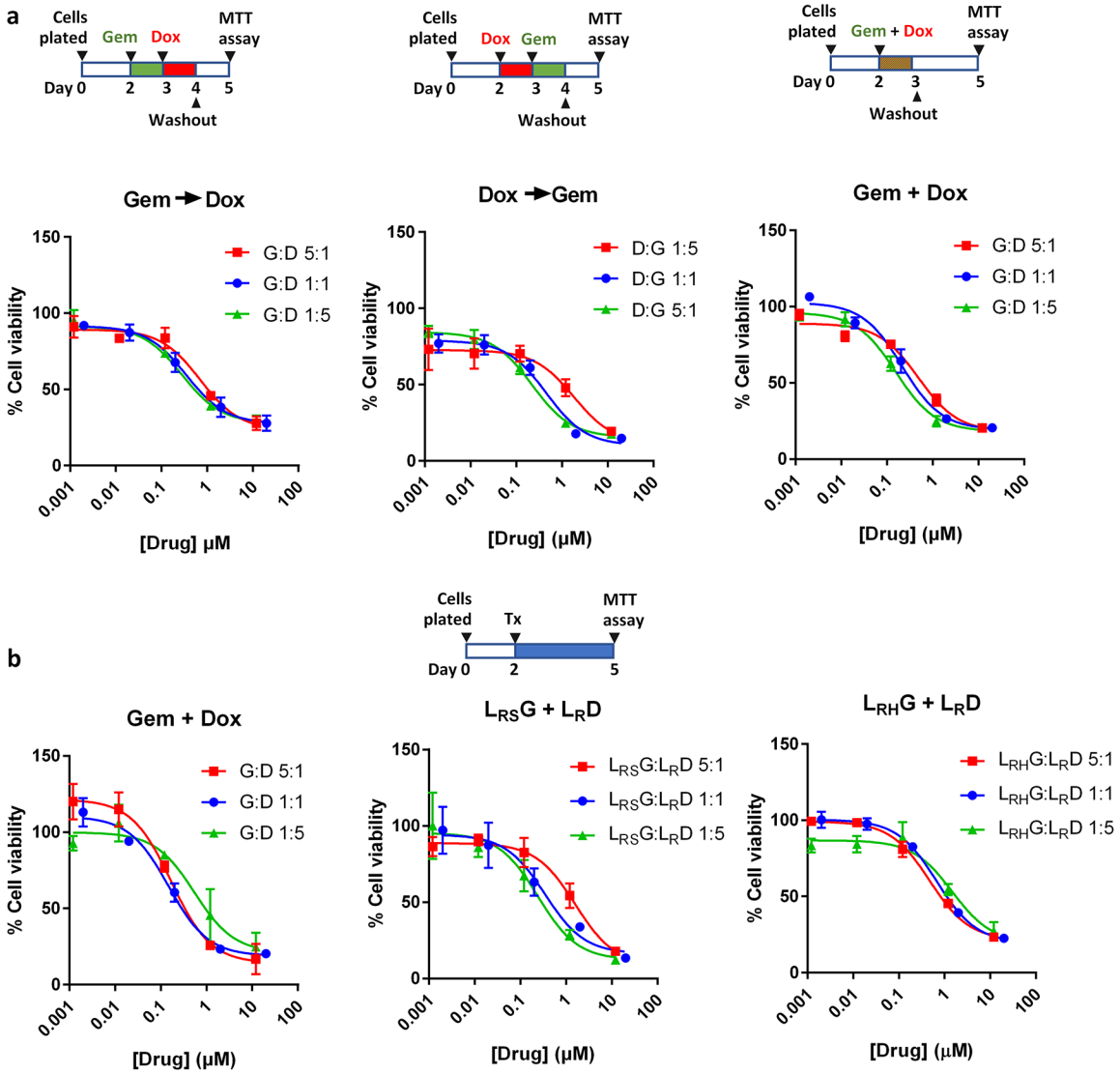

Fig. 7.

Cytotoxicity of (a) free Gem/Dox combinations on Huh7 cells given in different sequences and in different molar ratios (n = 3 tests. Mean ± s.d.) and (b) free or liposomal Gem/Dox combinations on Huh7 cells given simultaneously in different molar ratios (n = 3 tests. mean ± s.d.).

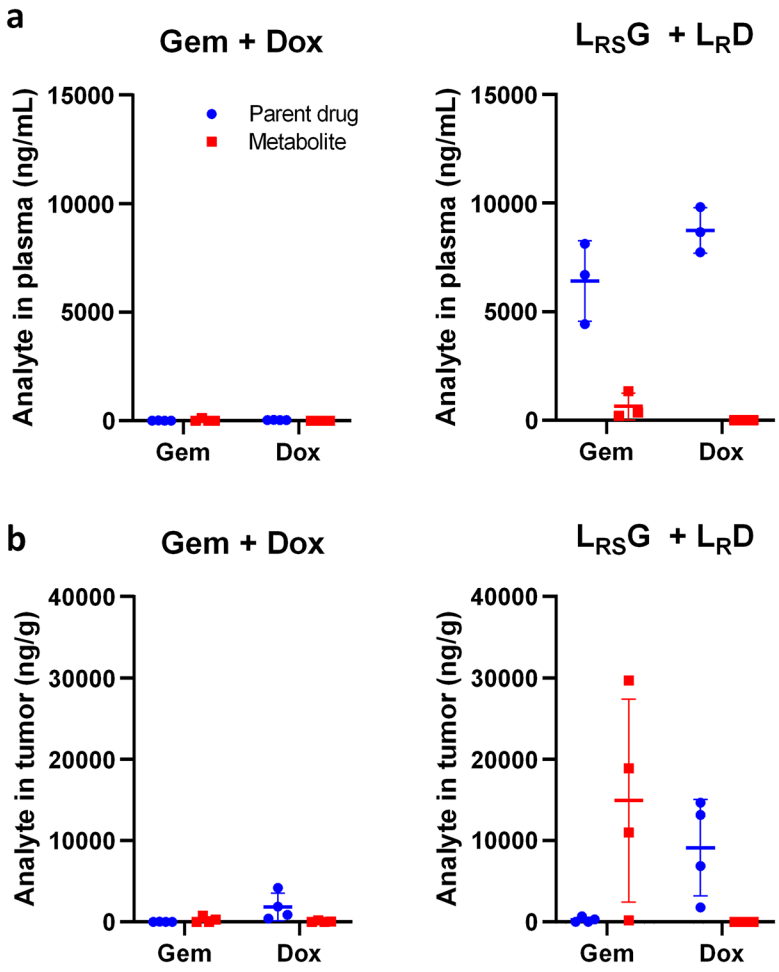

Fig. 8.

Drug concentrations in (a) plasma and (b) Huh7 tumors of animals treated with Gem + Dox free drug mixture or $L_{RS}G$ + L_RD liposomal mixture at 8 h post-IV injection. n = 4 expect for the plasma of liposomal mixture-treated group: n = 3.

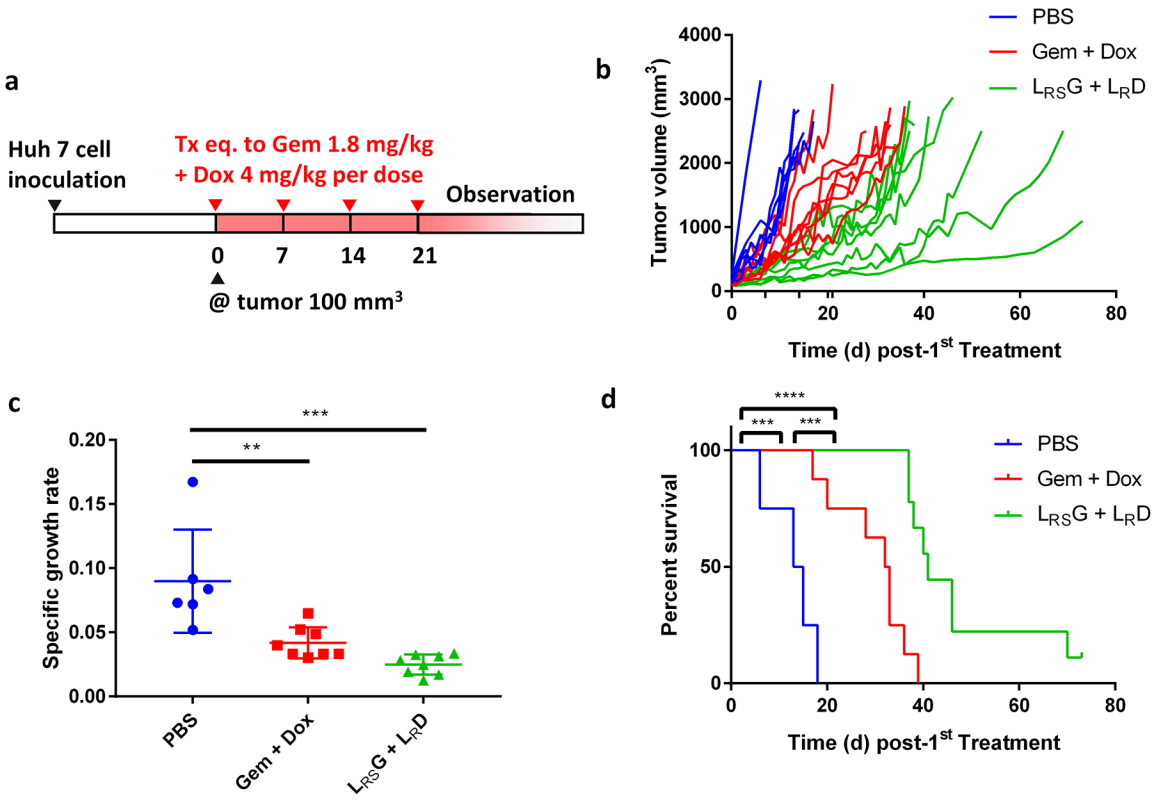

Fig. 9.

(a) Dosing schedule. (b) Changes of individual Huh7 tumor volume. Blue: PBS (n = 6); Red: Gem + Dox (n = 8); Green: $L_{RS}G + L_RD$ (n = 7). (c) Specific growth rate of Huh7 tumor: $\Delta \log V/\Delta t$ (V: tumor volumes; t: time in days). **: $p < 0.01$, ***: $p < 0.001$ by Tukey's multiple comparisons test. (d) Survival curve of the animals receiving PBS, Gem + Dox, or $L_{RS}G + L_RD$. ***: $p < 0.001$, ****: $p < 0.0001$ by Log-rank (Mantel-Cox) test.

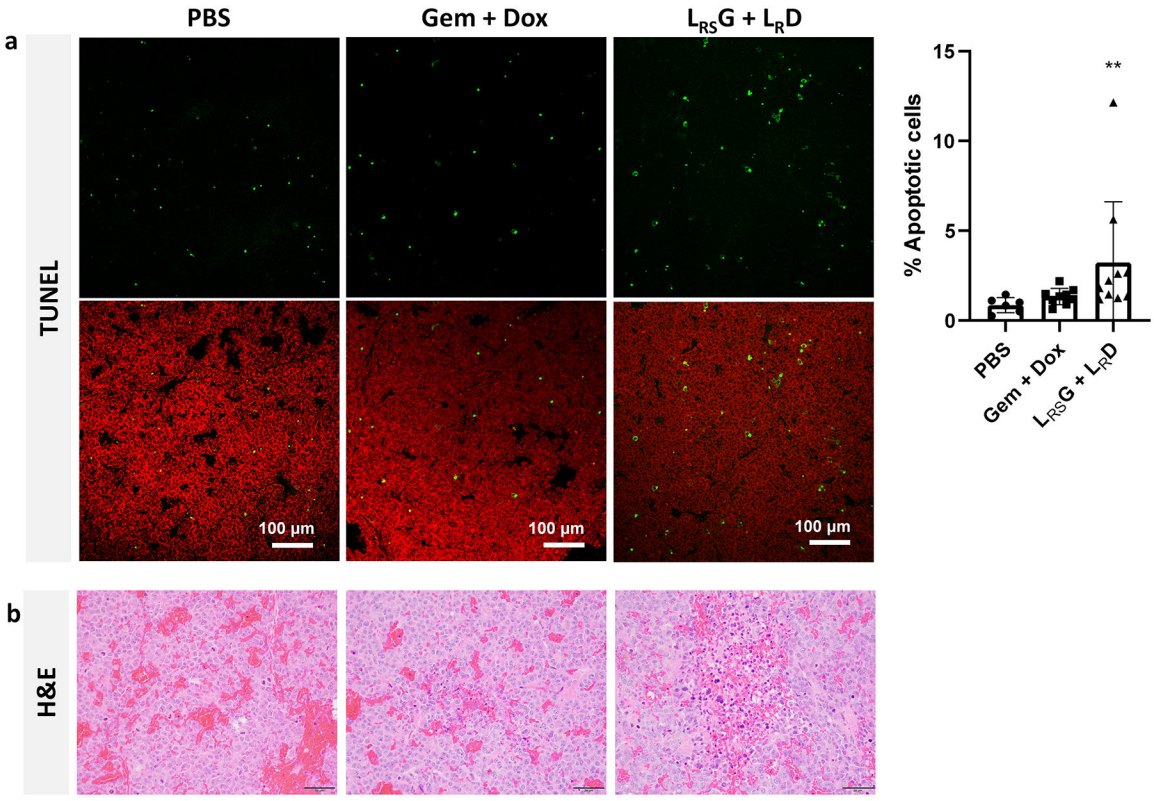

Fig. 10.

(a) Representative photographs of TUNEL-stained Huh7 tumor sections and quantitative analysis of TUNEL-stained sections. Top: TUNEL-stained apoptotic cells; Bottom: Composite images of TUNEL-stained apoptotic cells (green) and PI-stained nuclei (red); % apoptotic cells = number of apoptotic cells/total number of nuclei measured by a Nikon A1R confocal microscope (3–4 random fields per each tumor section). Scale bars: 100 μm. **: $p < 0.01$ vs. PBS by Dunn's multiple comparisons test following Kruskal-Wallis test. For all images, see Supporting Fig. 8; (b) Representative H&E stained Huh7 tumor sections. Scale bars: 50 μm. For other organs, see Supporting Fig. 9.

Table 1.

Physical properties of liposomes

Liposomes	Drug	Remote loading	Small volume loading	Hyper-tonic loading	Drug loading capacity (wt%)[a]	Encapsulation efficiency (wt%)[b]	Z-average (d, nm)	Zeta potential (mV)
$L_{RS}G$	Gem	+	+		9.4 ± 0.6	47.2± 2.8	217± 19	−29.6 ± 4.0
$L_{RH}G$	Gem	+		+	10.3 ± 1.4	52.2 ± 7.0	219 ± 18	−31.8 ± 2.6
$L_{R}D$	Dox	+			21.3 ± 2.5	106.5 ± 12.5	215± 16	−22.5 ± 3.3
$L_{RS}GD$	Dox	+	+		10.1 ± 2.1	60.6 ± 12.6	275 ± 1	−28.7 ± 3.2
	Gem				4.2 ± 1.0	25.2 ± 6.0		

[a]Drug loading capacity: Mass of loaded drug / mass of drug-loaded liposomes

[b]Encapsulation efficiency = Drug loading/theoretical drug loading × 100

Data are presented as means ± standard deviations of 3 tests of a representative batch.

Table 2.

Physical stability of liposomes during storage

Liposomes	Storage period (months)	Initial size (nm)	Size after storage at 4 °C (nm)	Initial zeta potential (mV)	Zeta potential after storage at 4 °C (mv)	% Drug Content *
$L_{RS}G$	1	218 ± 13	223 ± 2	−31.8 ± 2.6	−30.2 ± 1.8	98.1 ± 2.9
	2		208 ± 6		−26.6 ± 6.0	99.0 ± 1.8
	3		235 ± 1		−24.0 ± 1.6	98.8 ± 2.2
$L_{RH}G$	1	219 ± 19	220 ± 5	−29.6 ± 4.0	−32.1 ± 0.0	99.8 ± 3.0
	2		207 ± 8		−32.2 ± 1.0	101.5 ± 2.0
	3		197 ± 6		−25.5 ± 4.5	99.1 ± 1.0
$L_{R}D$	1	215 ± 16	210 ± 24	−22.5 ± 3.3	−22.0 ± 3.05	101.4 ± 1.2
	2		237 ± 4		−17.5 ± 0.9	98.9 ± 2.0
	3		259 ± 5		−14.5 ± 3.6	97.8 ± 1.0
$L_{RS}GD$	1	275 ± 1	906 ± 49	−28.7 ± 3.2	−11.9 ± 4.7	100.2 ± 1.0 (Gem) 98.7 ± 2.1 (Dox)

* % Drug content = Drug content after storage / initial drug content × 100

Data are presented as the averages ± standard deviations of 3 independently and identically prepared batches

Table 3.

Combination indices of free drug combinations

Molar ratio (Gem:Dox)	Gem → Dox (sequential)	Dox → Gem (sequential)	Gem + Dox (simultaneous)
5:1	0.55	0.62	0.17
1:1	0.77	0.89	0.62
1:5	0.56	0.56	0.53

Table 4.

Combination indices of liposomal drug combinations

Molar ratio (Gem:Dox)	$L_{RS}G + L_RD$	$L_{RH}G + L_RD$
5:1	0.25	0.68
1:1	0.3	0.42
1:5	0.29	0.22